

# **Fabrication of Copper Oxide Thin Films by the Drop Chemical Deposition Technique**

Muhammad Muhibbullah and Masaya Ichimura

Department of Engineering Physics, Electronics and Mechanics

Nagoya Institute of Technology, Gokiso-cho, Showa-ku, Nagoya 466-8555, Japan

## **Abstract**

Copper oxide thin films were deposited by the drop chemical deposition technique using an aqueous solution containing  $\text{CuSO}_4$  and  $\text{Na}_2\text{SO}_3$ . The deposited films were cubic crystalline structure and had O/Cu ratio of  $\sim 0.77$  with a very small amount of sulfur. The surface morphology of the films appeared compact without any crack. In the optical transmission measurement, a clear absorption edge was observed near 800 nm wavelength. Photo-electrochemical measurement confirmed the p-type conductivity and photosensitivity of the films.  $\text{Cu}_x\text{O}$ -based heterojunctions with ZnO were fabricated, and rectification properties and weak photovoltaic effects were observed.

Keywords: copper oxide; photosensitivity; thin films; chemical synthesis

## 1. Introduction

Copper oxide is advantageous for the photovoltaic application since its band gap is suitable for solar cells [1]. Furthermore, it has low toxicity and good environmental acceptability, and the constituent elements are both cheap and plentiful in nature. So far,  $\text{Cu}_2\text{O}$ -ZnO solar cells have been fabricated by various techniques. Minami et al. [2] and Mittiga et al. [3] fabricated the  $\text{Cu}_2\text{O}$  solar cell by oxidizing copper at high temperature. Some researchers have fabricated heterojunction using ZnO and  $\text{Cu}_2\text{O}$  both by electrochemical deposition (ECD) [4-8]. In addition, Ishizuka et al. fabricated ZnO/ $\text{Cu}_2\text{O}$  heterojunctions using magnetron sputtering [9].

Chemical techniques are increasing popular for synthesizing semiconductor particles, and there are many reports on particle synthesis of  $\text{Cu}_2\text{O}$  and other oxides [10-15]. In contrast, reports on chemical deposition of continuous thin films of  $\text{Cu}_2\text{O}$  are relatively few. Chemical bath deposition (CBD) is one of popular chemical techniques used for thin film deposition. There are several reports on CBD of  $\text{Cu}_2\text{O}$  continuous films [16-18], but the obtained thickness was too small for solar cell application in those previous works. In our previous work [19,20], to fabricate the ZnO- $\text{Cu}_x\text{O}$  heterojunction solar cells, copper oxide layers were deposited by CBD using a bath containing  $\text{CuSO}_4$  and  $\text{Na}_2\text{SO}_3$ . The substrate was immersed in the solution and situated horizontally at the bottom of the container. The thickness is large enough for an absorber layer of solar cells in our CBD, but the obtained films were porous and have rough surface morphology. In the present work, copper oxide  $\text{Cu}_x\text{O}$  layers are deposited by the drop chemical deposition (drop-CD) technique using aqueous solutions containing  $\text{CuSO}_4$  and  $\text{Na}_2\text{SO}_3$ . The substrate was placed on a heater plate, and then a small amount of the solution was dropped on it. As shown below, we can obtain  $\text{Cu}_x\text{O}$  films with a suitable thickness and fairly smooth surface morphology by drop-CD. We also observe that the films exhibit p-type conduction and photosensitivity. Preliminary results of  $\text{Cu}_x\text{O}$ -based heterojunction solar cells with ZnO as the counterpart are also given.

## 2. Experimental detail

The substrate used was indium-tin-oxide (ITO) coated glass sheet. The deposition solution contained 20 mmol/L  $\text{CuSO}_4$  and 100 mmol/L  $\text{Na}_2\text{SO}_3$  at an unadjusted pH of around 7.2 [20].  $\text{CuSO}_4$  was first dissolved in pure water, and then  $\text{Na}_2\text{SO}_3$  was added. The resulting solution was stirred for 30 min before the deposition. The solution was almost colorless after the stirring. The solution was then heated to around 65 °C. In our previous work [20], we found that the chemical reactions are activated at temperatures higher than 80°C, and thus the reactions are not yet active at 65°C. The substrate was heated on a separate heater plate until the desired temperature is reached. The heater plate temperature was varied from 130 to 170°C. A small amount of the solution was dropped on the substrate. The volume of a drop of the solution is about 0.05 mL, and the deposition area is about 0.64 cm<sup>2</sup>. The deposition process was done in cycle by performing the following steps: (a) a small amount of the solution is dropped on the heated substrate, (b) the substrate is washed softly using deionized water, (c) the substrate is heated again. The repetition of the deposition cycles was 30, and the deposition time per cycle was 2 min, unless otherwise stated. Finally, the deposited films were washed softly in pure water and dried naturally in air.

ZnO layers were deposited by electrochemical deposition technique (ECD) from an aqueous solution containing 100 mmol/L of  $\text{Zn}(\text{NO}_3)_2$  [21]. The deposition was performed in a conventional three-electrode cell with ITO substrate, saturated calomel electrode (SCE) and platinum sheet as working, reference and counter electrodes, respectively. These three electrodes were immersed in the solution. Solution pH was unadjusted (~4) and deposition voltage of -1.3 V was applied for 2 min. The solution was kept in a thermal bath at constant temperature of 60 °C throughout the deposition process. On the surface of the top layer of the  $\text{Cu}_x\text{O}$ -ZnO heterojunction, indium metal was deposited by vacuum evaporation. Both the substrate (In/ZnO/ $\text{Cu}_x\text{O}$ /ITO) and superstrate (In/ $\text{Cu}_x\text{O}$ /ZnO/ITO) heterostructures were fabricated and characterized.

An Accretch Surfcom-1400D profile meter was used to measure the thickness of the individual films and the heterojunctions. For compositional analysis, Auger electron

spectroscopy (AES) was carried out using a JEOL JAMP 9500F at a probe voltage of 10 kV and a current of  $2 \times 10^{-8}$  A. Argon ion etching was performed with an acceleration voltage of 3 kV and a current of 8 mA to sputter the film surface. The Cu/O atomic ratios were calculated using standard CuO. The X-ray diffraction (XRD) measurement was carried out by the RIGAKU RINT-2000 diffractometer using  $\text{CuK}\alpha_1$  radiation. The surface morphology of the film was analyzed using a Hitachi S-2000S scanning electron microscope (SEM) or JEOL JAMP 9500F at a constant acceleration voltage of 10 kV and a magnification of 2000. The optical transmission measurement was performed using the JASCO U-570 ultraviolet/ visible/ near infrared double beam spectrometer with the ITO substrate as the reference. Photoelectrochemical (PEC) measurements was done using 100 mmol/L  $\text{Na}_2\text{SO}_3$  aqueous solution and the three-electrode cell with saturated calomel electrode used as a reference electrode to determine the conduction type and estimate the photosensitivity of the  $\text{Cu}_x\text{O}$  films. The incident light from a xenon lamp (about  $100\text{mW}/\text{cm}^2$ ) was irradiated on the backside of the sample and it was turned off and on every 5 s in alternating manner. The current response was measured under the application of a ramp voltage with a scan rate of 5 mV/s. The photovoltaic properties of the fabricated  $\text{Cu}_x\text{O}$ -ZnO heterojunctions were measured under AM1.5 solar illumination with a power of  $100\text{ mW}/\text{cm}^2$ .

### 3. Results and discussion

Figure 1(a) shows the dependence of the film thickness on deposition time per cycle. The heater plate temperature was  $150\text{ }^\circ\text{C}$ , and the deposition cycle was 30. As depicted in the figure, the thickness increased with deposition time per cycle. After five minutes, the solution was almost vaporized. The film thickness also increases with the heater plate temperature as shown in Fig.1(b). The film was not deposited at heater plate temperatures below  $130\text{ }^\circ\text{C}$ . The solution started boiling at heater plate temperatures higher than  $170\text{ }^\circ\text{C}$ . The thickness is almost proportional to the number of the deposition cycles. Thus, the thickness is controllable by changing one of the three factors: deposition time per cycle, heater plate temperature, and number of deposition cycles. It should be noted that we can easily obtain films with a suitable

thickness for solar cell application using drop-CD technique. This result may signify that the method has an advantage over conventional CBD performed by other researchers[16-18].

Figure 2 shows the AES spectrum of the sample deposited at a heater plate temperature of 170 °C after sputtering the surface for 5 min. It is evident that copper and oxygen peaks were present in the spectrum with a small sulfur peak. The O/Cu and S/Cu ratios obtained from the AES spectra are shown in Table 1. In our previous work, no sulfur peak was observed in the AES spectra for the samples deposited by the CBD technique using the same  $\text{CuSO}_4$  and  $\text{Na}_2\text{SO}_3$  concentrations. The ratio of sulfur decreases with the heater plate temperature. There is no significant difference in the O/Cu ratio among the samples. The O/Cu ratio of the samples deposited by drop-CD is larger than that of conventional CBD-deposited samples [20]. Oxygen from the air may have significant contribution to the obtained O/Cu ratio in the drop-CD process.

Figure 3 shows the XRD spectra for the films deposited at different heater plate temperature. Some peaks due to ITO were observed, and all other dominant peaks are attributed to  $\text{Cu}_2\text{O}$  according to the ICSD standard data. Thus the XRD results show that the films are dominantly crystalline  $\text{Cu}_2\text{O}$ , although  $\text{Cu}/\text{O} < 2$  according to the AES results.

Figure 4(a) is the SEM photograph for the films deposited by the conventional CBD techniques [20]. The solution composition is the same as that used in the drop-CD method, The heater plate temperature is 200 °C and the deposition time 30 min. As shown in the figure, the film consists of many octahedral particles on a substrate. Chemical syntheses of similar octahedral or cubic particles have been reported in literatures [12-15]. Figures 4(b), (c) and (d) are the photographs for the films deposited using the drop-CD technique at the heater plate temperature of 140, 150 and 170 °C, respectively. The drop-CD films are much more compact than the sample deposited by CBD. In our previous CBD process, the particles can grow with continuous supply of ions from the bulk of the solution. In contrast, in drop-CD, the particle size is reduced because the amount of ions in the solution dropped on the substrate is limited. Thus the films consist of small particles and are much more dense than the CBD film.

The typical optical transmission spectrum of the film deposited by drop-CD is shown in Fig.

5(a). The film was deposited at 150 °C heater plate temperature and its thickness is 2.5 μm. On the other hand, a relatively thicker (5 μm) film was obtained at 170 °C and its transmission is low in the infrared to ultraviolet region. For a direct band gap material, the band gap energy can be calculated using the relation  $\alpha = k(h\nu - E_g)^{1/2}/h\nu$ , where  $k$  is a constant,  $E_g$  is the band gap and  $h\nu$  is the photon energy. The relation between  $h\nu$  versus  $(\alpha h\nu)^2$  plotted in Fig. 5(b) does not follow the simple relation, and it seems that two straight line portions could be considered. One corresponds to the band gap of about 1.4 eV and the other about 2 eV. The former is within the range of the reported band gap values of CuO, and the latter is near to the literature value of the Cu<sub>2</sub>O band gap. This seems to be consistent with the AES results that the composition is in between CuO and Cu<sub>2</sub>O. In our previous work on CBD of Cu<sub>x</sub>O, no clear absorption edge was observed because of scattering of light due to the very porous structure as shown in Fig.4(a). By adopting the drop-CD, the morphology of the film is improved (more compact) and hence, a clear absorption edge appears as can be seen in Fig. 5(a).

Figure 6 shows the PEC measurement results for the films deposited with the heater plate temperature of (a) 150 °C, and (b) 170 °C. It is clear that the current was changed due to the light chopping, and thus the films show good photosensitive behaviors. Under illumination, some carriers were excited in the illuminated region of the film. Then excited minority carriers diffused to the surface during their lifetime to participate in the electrochemical reaction at the electrolyte interface. For our thin films, the negative photocurrent under cathodic bias is larger than the positive photocurrent under anodic bias. This implies that the minority carriers are electrons, and thus the deposited films exhibit p-type conductivity. The photocurrent is larger for the film deposited at a higher heater plate temperature (Fig.6(b)). In Fig.6(a), the positive photocurrent was only slightly smaller than the negative photocurrent. Thus, although the conduction type is p-type, its hole concentration could be low.

Fig. 7 shows I-V characteristics for the superstrate structure in which Cu<sub>x</sub>O deposited at (a) 150 °C and (b) 170 °C heater plate temperatures. Deposition cycles were 10 for (a) and 8 for (b), and the thickness was around 1 μm for both samples. Deposition time of the ZnO layers

was 2 min and the thickness was around 1.5  $\mu\text{m}$ . Some portion of the ZnO layer dissolved during the deposition of the  $\text{Cu}_x\text{O}$  layer. Thus, it is somewhat difficult to exactly determine the thickness of  $\text{Cu}_x\text{O}$  and ZnO layers after the fabrication of the heterojunction. There is no rectification property for the superstrate structure with  $\text{Cu}_x\text{O}$  layer deposited for 20 or more cycles. The solar conversion efficiency is  $4 \times 10^{-4} \%$  with  $V_{oc} = 0.052 \text{ V}$ ,  $I_{sc} = 2.6 \times 10^{-2} \text{ mA/cm}^2$  and F.F. = 0.29, and  $1.2 \times 10^{-3} \%$  with  $V_{oc} = 0.054 \text{ V}$ ,  $I_{sc} = 8.7 \times 10^{-2} \text{ mA/cm}^2$  and F.F. = 0.26 for heterojunctions fabricated using  $\text{Cu}_x\text{O}$  deposited at 150 and 170°C heater plate temperature, respectively. The heterojunction with  $\text{Cu}_x\text{O}$  layer deposited at 170°C heater plate temperature showed higher solar conversion efficiency compared to the heterojunction with  $\text{Cu}_x\text{O}$  layer deposited at 150°C. This would be consistent with the obtained PEC results where the photocurrent is larger for the  $\text{Cu}_x\text{O}$  film deposited at 170°C. On the other hand, the poor rectification property and no photovoltaic effect were observed in the substrate structure of  $\text{Cu}_x\text{O}$ -ZnO heterojunction. Although compact  $\text{Cu}_x\text{O}$  films were obtained by adopting drop-CD technique, properties of the  $\text{Cu}_x\text{O}$ -ZnO heterostructures are still poor. One of the reasons could be the dissolution of the first layer during the second layer deposition. Therefore, heterojunctions with other n-type materials other than ZnO need to be considered and examined.

#### 4. Conclusions

$\text{Cu}_x\text{O}$  thin films were deposited by the drop-CD technique using  $\text{CuSO}_4$  and  $\text{Na}_2\text{SO}_3$ . The AES measurements revealed that O/Cu ratio was approximately 0.77 with small amount of S. The XRD measurements showed that the  $\text{Cu}_x\text{O}$  films are dominantly cubic crystalline  $\text{Cu}_2\text{O}$ . The optical transmission measurements revealed the clear absorption edge near 800 nm. The films exhibited p-type conduction with photosensitivity.  $\text{Cu}_x\text{O}$ -ZnO heterojunctions were fabricated with ZnO layers deposited by electrochemical deposition. Rectification properties and weak photovoltaic effects were observed for heterojunctions with the superstrate structure. The technique employed in this work is a low cost technique, which used inexpensive source chemicals and a simple apparatus. Therefore, the drop-CD technique is potentially suitable for

commercial production of solar cells.

### **Acknowledgements**

We would like to thank Dr. Masashi Kato for his helpful discussion, and Mr. Junie Jhon M. Vequizo for improving the manuscript.



## References

- [1] A. E. Rakhshani, Solid-State Electronics, 29 (1986) 7.
- [2] T. Minami, Y. Nishi, T. Miyata, and J. Nomoto, Appl. Phys. Exp. 4 (2011) 062301.
- [3] A. Mittiga, E. Salza, F. Sarto, M. Tucci, and R. Vasanthi, Appl. Phys. Lett. 88 (2006) 163502..
- [4] M. Izaki, T. Shinagawa, K. Mizuno, Y. Ida, M. Inaba, and A. Tasaka, J. Phys. D 40 (2007) 3326.
- [5] J. Katayama, K. Ito, M. Matsuoka and J. Tamaki, J. Appl. Electrochem., 34 (2004) 687.
- [6] S. S. Jeong, A. Mittiga, E. Salza, A. Masci and S. Passerini, Electrochimica Acta, 53 (2008) 2226.
- [7] T. Jiang, T. Xie, Y. Zhang, L. Chen, L. Peng, H. Li and D. Wang, Phys. Chem. Chem. Phys., 12 (2010) 15476.
- [8] M. Ichimura and Y. Song, Jpn. J. Appl. Phys., 50 (2011) 051002.
- [9] S. Ishizuka, K. Suzuki, Y. Okamoto, M. Yanagita, T. Sakurai, K. Akimoto, N. Fujiwara, H. Kobayashi, K. Matsubara and S. Niki, Phys. Stat. Sol., (c) 1 (2004) 1067.
- [10] Y. Zhai, H. Fan, Q. Li, and W. Yan, Appl. Surf. Sci., 258 (2012) 3232.
- [11] W. Yan , H. Fan, and C. Yang, Mater. Lett., 65 (2011) 1595.
- [12] Y. Sui, W. Fu, H. Yang, Y. Zeng, Y. Zhang, Q. Zhao, Y. Li, X. Zhou, Y. Leng, M. Li, and G. Zou, Cryst. Growth Design, 10 (2010) 99.
- [13] F. Du, J. Liu, and Z. Guo: Mater. Res. Bull. 44 (2009) 25.
- [14] L. Gou and C. J. Murphy: Nano Lett. 3 (2003) 231.
- [15] S. Sun, F. Zhou, L. Wang, X. Song, and Z. Yang, Cryst. Growth Design, 10 (2010) 541.
- [16] M. Ristov, G. I. Sinadinovski and I. Grozdanov, Thin Solid Films, 123 (1985) 63.
- [17] M. T. S. Nair, L. Guerrero, O. L. Arenas and P. K. Nair, Appl. Surf. Sci., 150 (1999) 143.
- [18] J. Medina-Valtierra, S. Calixtob, F. Ruiz, Thin Solid Films, 460 (2004) 58.
- [19] M. Muhibbullah and M. Ichimura, Trans. Mater. Res. Soc. Japan, 36 (2011) 195.
- [20] M. Muhibbullah and M. Ichimura, Jpn. J. Appl. Phys., 49 (2010) 081102.
- [21] M. Izaki, J. Electrochem. Soc. 144 (1997) 1949.

### **Figure captions**

Fig. 1: Thickness of the  $\text{Cu}_x\text{O}$  thin film as a function of (a) deposition time per cycle and (b) heater plate temperature.

Fig. 2: AES spectrum of the  $\text{Cu}_x\text{O}$  thin film deposited at 170°C heater plate temperature.

Fig. 3: XRD of the  $\text{Cu}_x\text{O}$  films prepared with different heater plate temperatures.

Fig. 4: SEM photographs of the  $\text{Cu}_x\text{O}$  films deposited (a) by the conventional CBD technique and at (b) 140°C, (c) 150°C and (d) 170°C heater plate temperature using the drop-CD technique.

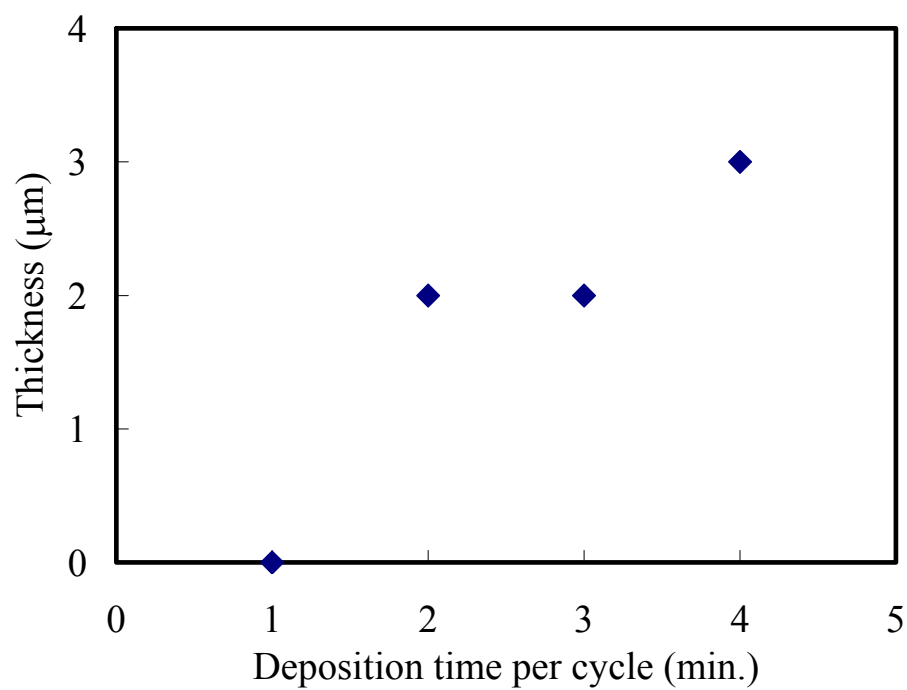
Fig. 5: (a) optical transmission and (b) the plot for calculation of the band gap for the  $\text{Cu}_x\text{O}$  film deposited at 150°C.

Fig. 6: PEC measurement results for the  $\text{Cu}_x\text{O}$  films deposited at (a) 150°C and (b) 170°C heater plate temperature.

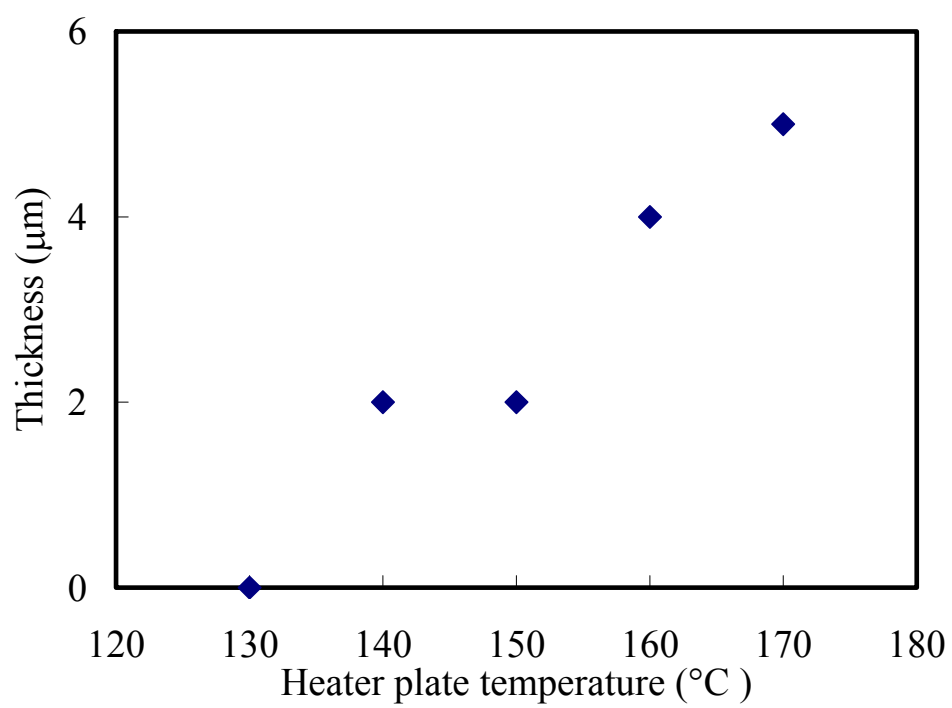
Fig. 7: I-V characteristics for the superstrate-structure heterojunctions in which the  $\text{Cu}_x\text{O}$  layer was deposited at (a) 150 °C and (b) 170 °C heater plate temperature.

Table 1 : Composition of the Cu<sub>x</sub>O thin films deposited with different deposition conditions. The standard condition is deposition time per cycle: 2 min, heater plate temperature: 150°C, Na<sub>2</sub>SO<sub>3</sub> concentration: 100 mmol/L, and one of the parameters was varied for each set. (The repetition number is 30.)

Parameters of the deposition		Composition ratio Cu : O : S
Deposition time per cycle (min.)	2	1 : 0.77 : 0.055
	3	1 : 0.78 : 0.039
	4	1 : 0.75 : 0.046
Heater plate temperature (°C)	140	1 : 0.78 : 0.042
	150	1 : 0.77 : 0.055
	160	1 : 0.77 : 0.035
	170	1 : 0.78 : 0.026
Na <sub>2</sub> SO <sub>3</sub> concentration (mmol/L)	80	1 : 0.72 : 0.05
	100	1 : 0.77 : 0.055
	120	1 : 0.83 : 0.039



(a)



(b)

Fig. 1

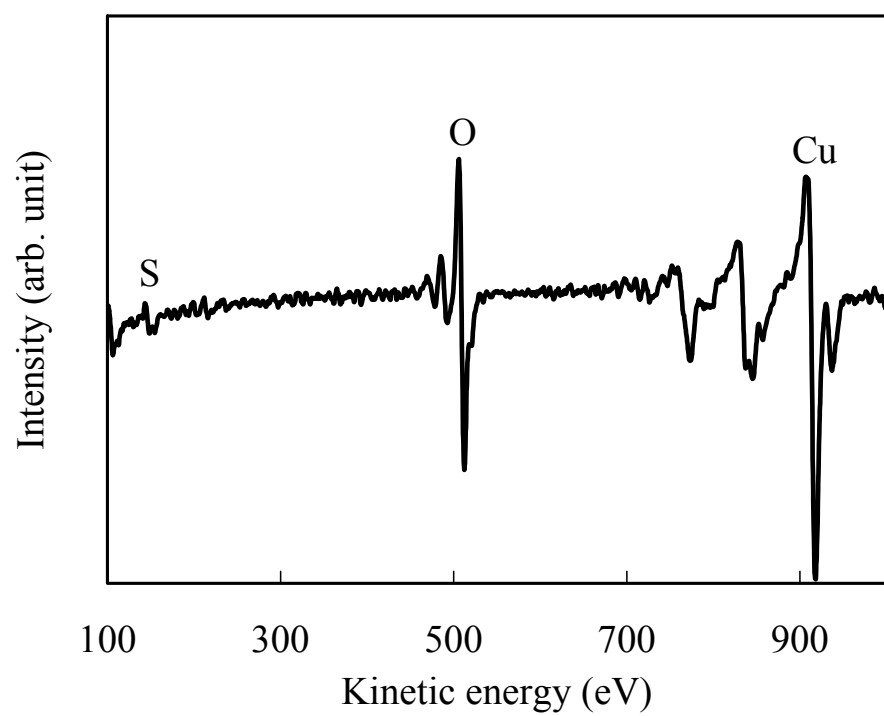


Fig. 2

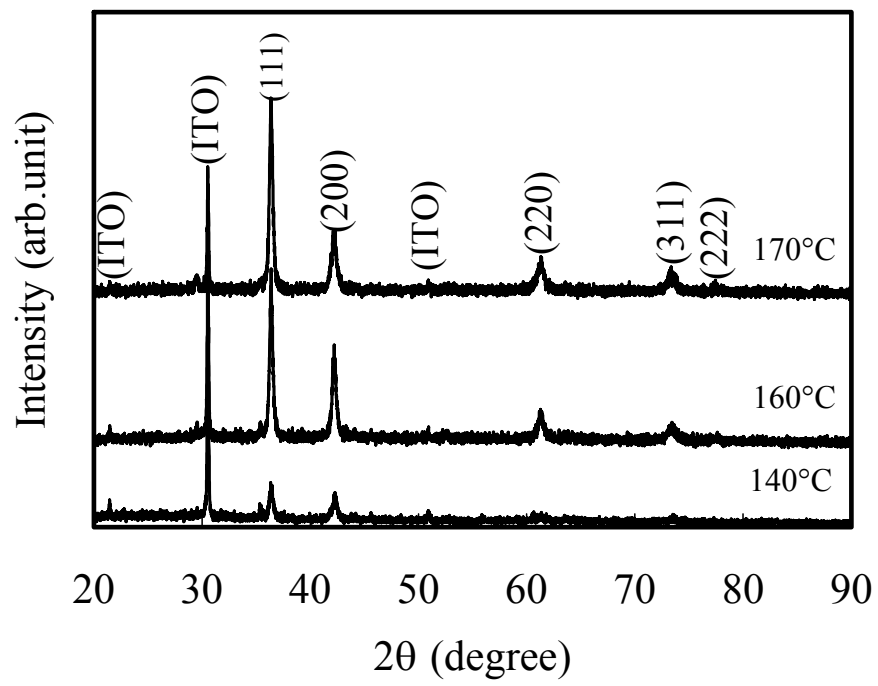
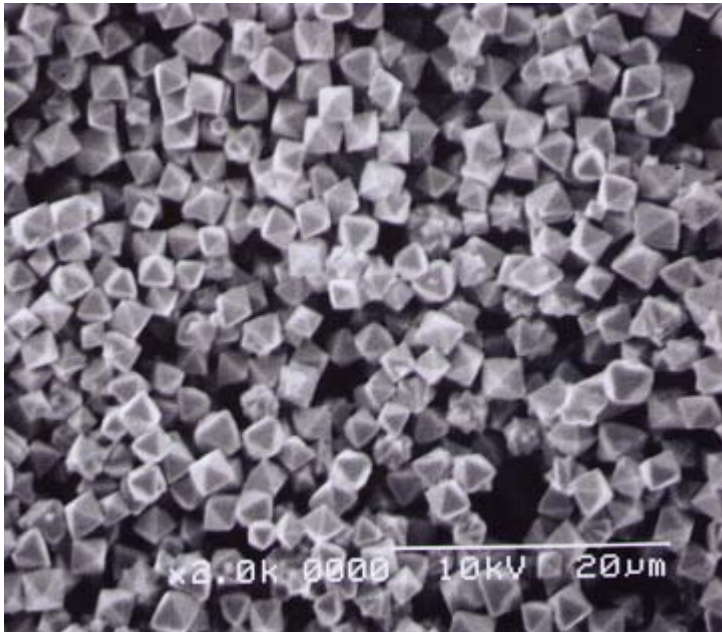
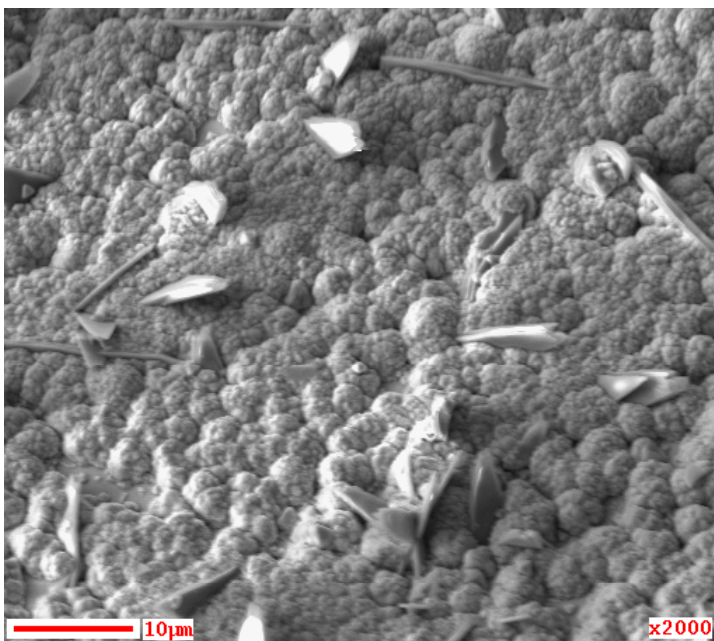


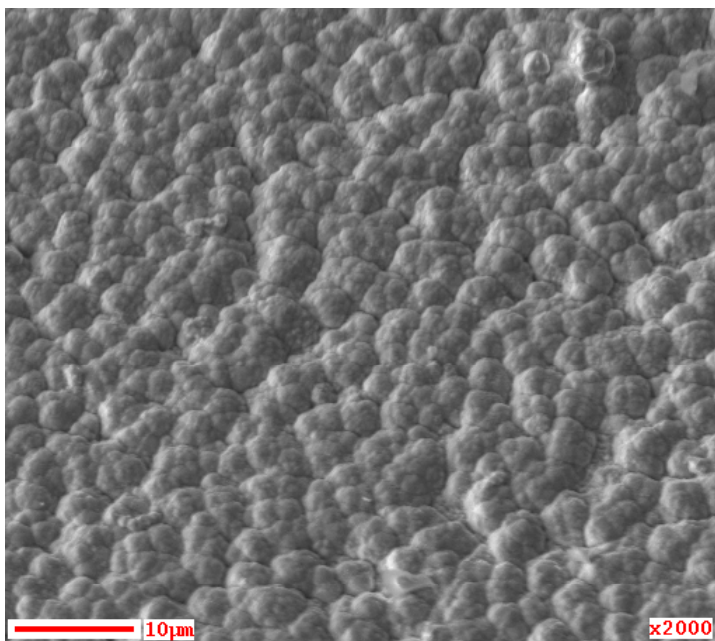
Fig. 3



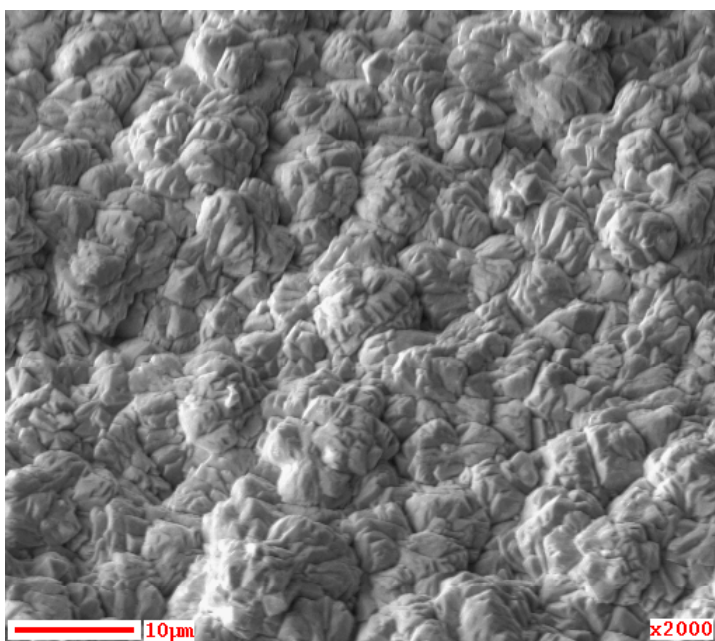
(a)



(b)



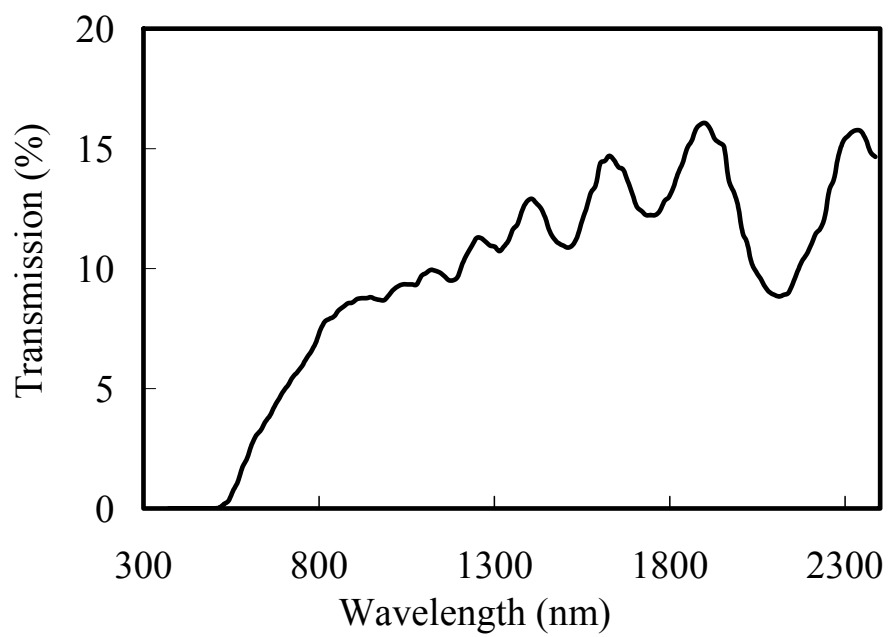
(c)



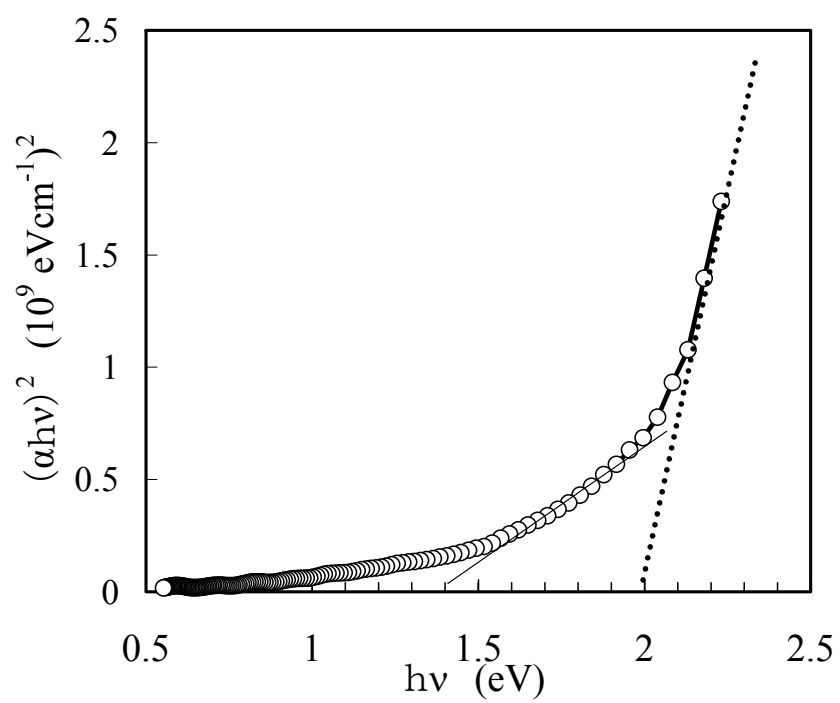
(d)

Fig. 4



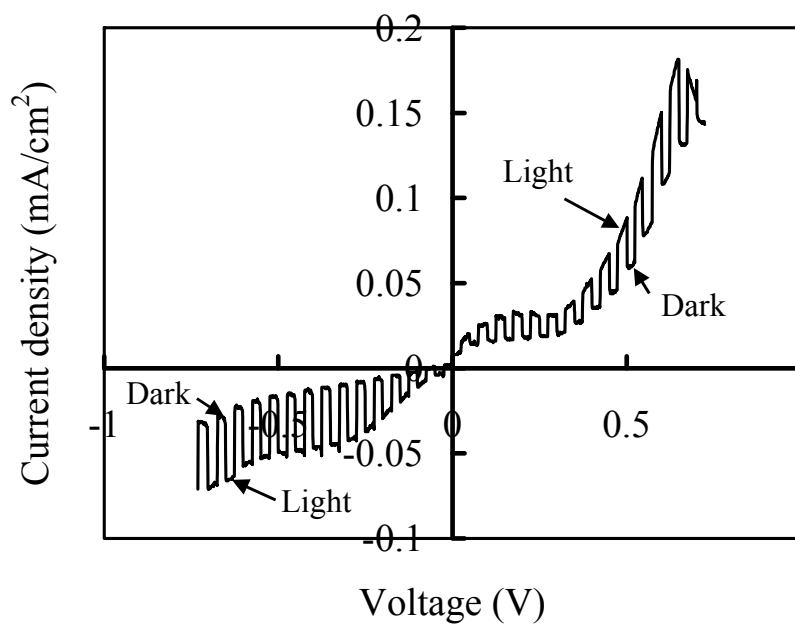


(a)

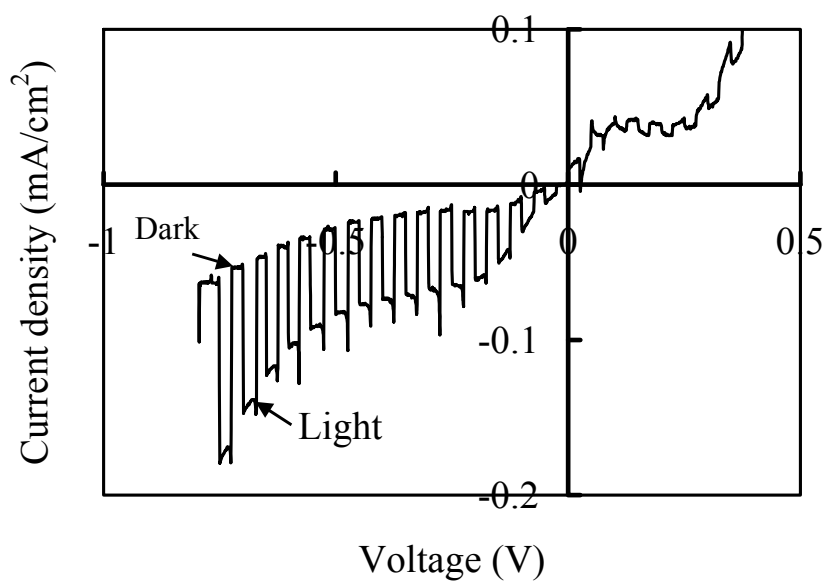


(b)

Fig.5

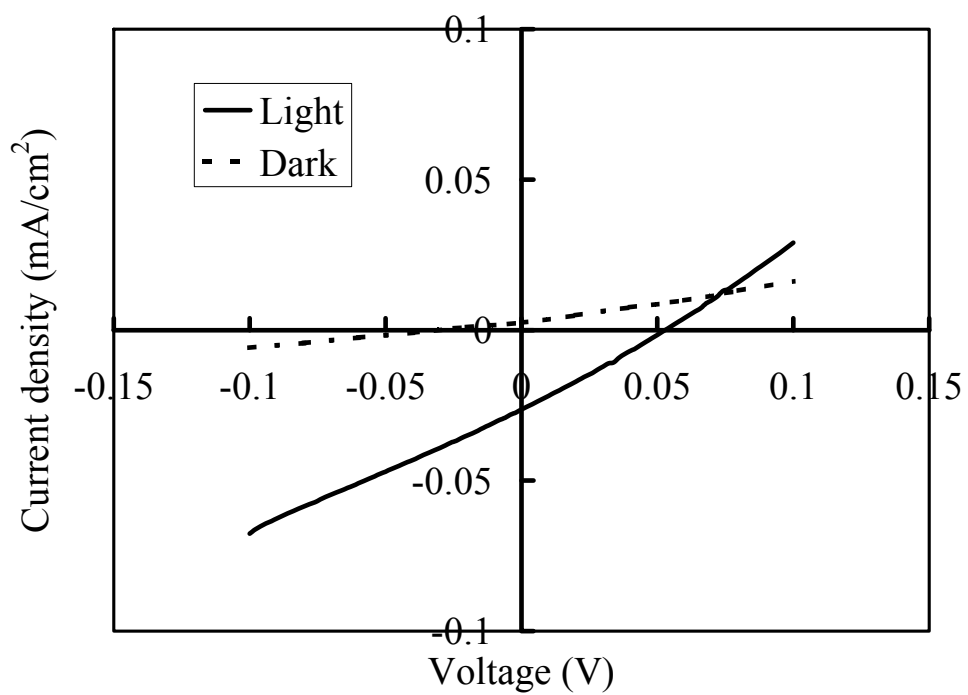


(a)

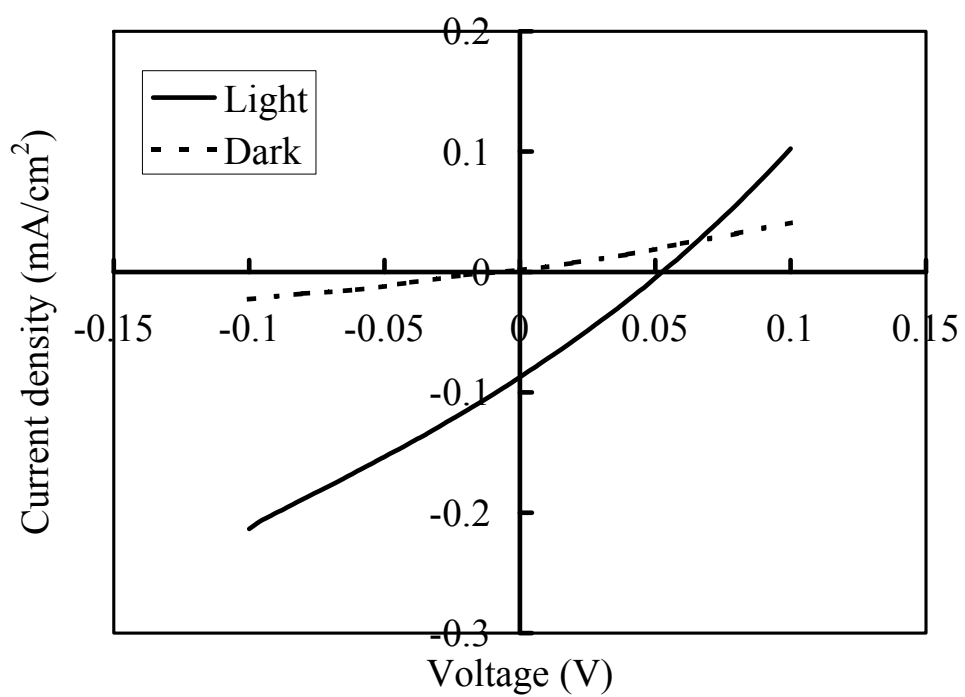


(b)

Fig. 6



(a)



(b)

Fig. 7